A PROBABILISTIC SEISMIC ANALYSIS OF CONTAINMENT LINER INTEGRITY

M. N. FARDIS, C. A. CORNELL
Department of Civil Engineering, Massachusetts Institute of Technology,
J. E. MEYER
Department of Nuclear Engineering, Massachusetts Institute of Technology, Cambridge, Massachusetts 02139, U.S.A.

SUMMARY

After determining the dynamic response of the containment to seismic events well beyond the Safe-Shutdown-Earthquake, the integrity of the liner under the induced stresses is assessed.

In a containment composed of a concrete structure with a steel liner plate attached to its interior face, the liner's function is to isolate the containment atmosphere from the environment, even in case the concrete is cracked. To perform this function the liner must be absolutely leak-tight.

The response to Earthquake ground motion is found by representing the containment as a distributed mass beam, and considering only the first vibrational mode. Depending on the extent of cracking, the response will be between that of a shear beam and that of a cantilever beam. The stresses at any point are found then from internal forces, as a combination of the stresses from a shell model (with mainly membrane action) and the stresses from a beam model, in which horizontal planes remain plane. The resulting stresses and strains in the liner reveal that although the liner might yield under very high ground accelerations, its high ductility will prevent it from tearing.

As the average performance of the liner will be satisfactory, we next seek potential localized weak points in it. We identify the seam welds between adjacent liner panels as such points, and weld defects as potential crack initiators.

Statistics concerning the size and frequency of occurrence of weld defects in structures similar to the liner plate are used. Assuming that the provisions of the ASME-ACI code, regarding sampling and radiographe examination of welds, are applied, we find the frequency of occurrence of various sizes of defects after examination and the cold-pressure-test.

A defect of given size may become a crack initiator by either brittle fracture or ductile rupture. By using: (1) linear elastic fracture mechanics, (2) experimental results regarding the dynamic fracture toughness of similar steel plates, (3) a probability distribution of the liner temperature under operating conditions, and (4) a probability distribution of the Liner Nil-Ductility-Transition Temperature, we find the probability that a given size defect will fracture under given stress. We also find the probability of ductile rupture under given strain, which is found to be negligibly small in comparison to the probability of brittle fracture.

By combining the results above we find the probability that a weld point will become a crack initiator under given stress. Assuming independence of weld occurrence, and under given state of stress on the entire liner, the number of crack initiators is Poisson distributed.

We make use of statistics regarding the distribution of the peak ground acceleration over different horizontal directions. We also include the uncertainty in the structural model. By combining these we find the probability distribution of various states of stress over the entire liner, for given recorded peak ground acceleration.

The result is the probability distribution of the number of crack initiators, and the probability distribution of the total crack length, as a function of peak ground acceleration.

1. Introduction

Containment structures for nuclear power plants are designed to withstand "service", "severe environmental" and "extreme" loads. Although the "extreme" design loads are chosen so as to have a very low probability of occurrence, the question of what happens at loads higher than the extreme design loads does arise.

A reliability study has been undertaken, which, by using simple methods, aims at giving some insight into the behavior of containments under the very unlikely event of a loading condition beyond the extreme design loads. In this paper we attempt to estimate the damage to the containment liner caused by these higher loads.

It is common U.S. practice to achieve accident leak-tightness of concrete containment structures by attaching a thin steel plate, the liner, to the entire inside face of the concrete shell by the use of anchors*. The strains in the liner are determined from the relative displacements of adjacent anchors. The anchor spacing is approximately the same as the average spacing of the concrete-cracks (which are formed during the cold-pressure test). Therefore, the strains in the liner under any loading condition deviate only slightly from the concrete wall average strains (in which the concrete cracks effect has been smeared).

The liner material typically has a low yield stress and an extremely high ductility. The strains in the liner under internal accident conditions (but below overpressurization) and under seismic excitations (even of intensity far beyond the Safe Shutdown Earthquake) are not capable of causing tearing of this--on the average--very ductile material. Therefore, to find the conditions under which the liner may lose its integrity, we try to characterize weak (i.e., flawed) points in it.

The welds between adjacent liner panels may become the weak link due to a combination of geometric discontinuities, such as flaws, and of metallurgical damage in the heat affected zone and the weld metal. The weld metals commonly used are at least equally as ductile and tough as the parent metal, and a proper welding process and design may ensure excellent performance of the welded liner plate, provided that it is flaw-free. Liner cracks, however, may initiate at flawed locations in the welds under stress. A statistical study of the occurrence of defects and of their effects on the liner integrity becomes then necessary.

Cracks in the liner are important because, when they are combined with through-thickness cracks in the concrete wall, they represent potential release routes for the possibly contaminated containment atmosphere during an accident. The high liner temperature during an internal accident, however, increases the material toughness enough to prohibit crack initiation and propagation even from metallurgically damaged locations. Therefore, the liner cracks must pre-exist. The reason, then, we investigate crack formation in the liner under seismic conditions is that this is the only case that high stresses may develop over a major part of the liner membrane, under non-internal accident conditions. Furthermore, the liner temperature may be cold enough to permit crack initiation and propagation.

---

*For the work of this paper the effect of any wall (and liner) penetrations is neglected, i.e., an idealized containment structure is considered with continuous liner and concrete wall at the penetration locations.

2. Crack Formation for a Known Local Stress

The immediate objective is to find the probability that from a point in the liner plate under given stress and strain conditions a crack will initiate and propagate. As explained in the introduction, this probability is nonzero only for defective weld locations. The problem reduces to: 1) the establishment of the mean rate of occurrence of defects of size above a lower bound incapable of producing a crack under any conditions; 2) the probability distribution of sizes of defects above the afore-mentioned lower bound, conditional on the occurrence of defects above this bound; 3) the establishment of failure modes and associated failure criteria at defective locations; and 4) the utilization of the failure criteria to obtain the probability of crack initiation and propagation from a defect of given size and under given local stress conditions.

We will pursue the above points in turn:

To determine the rate of occurrence of defects above a lower bound of interest we make use of the only relevant data available to us: the rate of defect occurrence in radiographs of welded members in Japanese ship structures. These data are drawn from an extensive study (Kihara et al 1960) and refer to steel plates of thicknesses and materials similar to those commonly used for containment liners, welded under similar conditions. The form in which these data have been presented is dictated by the way the Japanese specifications JIS Z2341 for radiographic inspection group defects into 6 Classes according to their size and number found in a 10mm x 50mm weldment "reference area" (Class 1 means no defects and Class 6 includes the most severe defects). Accordingly, the data in Kihara et al (1960) give the relative frequency of occurrence of Class i (i = 1 to 6) defects.

After transforming the weldment "reference area" of the Japanese specification into a weldment "reference length" ℓ_o, we adopt the frequency distribution of defect Classes as the probability mass function of defect Classes for the population of weldments of this type. Therefore, we assume that it is representative of the existing defects in any "reference length" ℓ_o of a liner weldment prior to insitu inspection and repair.

Radiographic examination is typically applied for liner welds. The ASME-ACI code for concrete components in Nuclear Service (ASME, 1974) specifies a certain radiographic inspection procedure and acceptance criteria. Roughly all defects in JIS Classes 4 to 6 are considered unacceptable by this code. As far as the inspection procedure is concerned, the code specifies that the weldment is divided into weld test units of length ℓ_u equal to 50 ft (15m) and for each one of them a sample length ℓ_t equal to 1 ft (0.30m) is fully radiographed. Certain actions are taken depending on the outcome of the inspection of this first ℓ_t length, as shown in Fig. 1 in the form of an event tree.

We adopt some values for inspection and repair efficiencies (Fardis, 1977) and we make the key assumption of independence of occurrences and sizes (i.e., Classes) of defects at non-overlapping weld "reference lengths". We can then find the probability mass function of the existing defect Classes in a weld "reference length" after inspection according to the code, and repair (Fardis, 1977).

It is easy to identify Class 6 defects as the only potential cause of loss of liner integrity under any conditions. It is also possible to establish from Kihara et al (1960) the lower bound of Class 6 defect sizes.

Once we have established the mean rate of occurrence of Class 6 defects per weld "reference length" and once we have identified these defects as the only ones of interest, we proceed in establishing a probability distribution of Class 6 defect sizes. As far as the representative size D of an individual defect with an idealized ellipsoidal shape is concerned, we choose to represent it by a shifted truncated exponential distribution with a lower bound of 0.08 in. (Kihara et al 1960), an upper bound equal to the liner thickness, and a parameter β equal to 3 in.$^{-1}$(120m^{-1}). As far as the aggregate cross-sectional area DA of a cluster of defects (expressed as a fraction of the weld cross-sectional area) is concerned, we choose to represent it also by a truncated shifted exponential with a lower bound of 0.08 (Kihara et al 1960) and a parameter β of 3. The upper bound is chosen to result in very small probabilities of crack initiation in the entire liner during the cold-pressure test: for a typical PWR containment this upper bound was established equal to 85%.

Finally, in addition to the spatial independence assumption, we assume that at most one Class 6 defect may exist in each weld "reference length".

The failure (i.e., crack initiation) modes considered were brittle fracture and ductile rupture.

The failure criterion adopted for brittle fracture was the simple criterion of Linear Elastic Fracture Mechanics:

$$K_{ID} \leq Q \sqrt{\pi a}\, \sigma \qquad (1)$$

The use of this criterion implies idealization of the defect geometry as an ellipsoid. We further adopt an average aspect ratio of this ellipsoidal shape, which determines the shape parameter Q. a is proportional to a characteristic size D of the individual defect (the (conditional) probability distribution of which has been established above). The major tensile principal stress is used for the uniaxial stress σ. The experimental results by Shoemaker et al (1969) and by Shabbits (1970) on the dynamic toughness of steels, have been utilized to obtain the dynamic material toughness K_{ID} as a piecewise linear function of (T-NDTT). Based on the data available to us we adopt a normal distribution N (100, 10^2)* for the liner temperature T under normal (i.e., non-accident), conditions, and a normal N (0, 20^2) for the Nil Ductility Transition Temperature, NDTT, of both the parent and the weld metal. The numerical values of the parameters in parentheses are in degrees Farenheit. The corresponding values in degrees Celsius are N (38, 6^2) and (-18, 11^2).

Based on the criterion in eq. (1) and on an approximate modification of it for the inelastic stress region (Fardis 1977) we can obtain the probability that a crack will initiate from a defect of size D under local stress (symbolically $P(b|D,\sigma)$). Brittle crack initiation means unstable crack propogation in the medium, as well, as long as a drastic drop in stress does not occur.

The following failure (i.e., crack initiation) criterion for ductile rupture is suggested by experimental results: for given defect cluster aggregate area DA (the (conditional) probability distribution of which has been described previously) the average liner strain required to cause failure is lognormally distributed with a standard deviation equal to

*We denote a normal distribution with mean m and variance σ^2 by N(m, σ^2).

2% (strain) and a mean linearly dependent on DA in the following way: it takes on the value 0 for DA equal to 90.7% (a value that corresponds to the aggregate area of uniform, closely packed spherical defects) and it takes on a value equal to the average total elongation of the weld metal (referring to a gage length equal to the liner anchors spacing) for DA equal to 0.

Crack initiation by ductile rupture does not mean in general unstable crack propagation. The Fracture Analysis Diagram (Pellini, 1971) describes the stress and temperature T conditions under which an initiated crack will propagate in a medium of known NDTT. Using the probability distributions of T and NDTT, the crack initiation by ductile rupture criterion, and the Fracture Analysis Diagram, we can find the probability of crack propagation by ductile rupture from a defect of given "size" DA, under known stress (σ) and strain (ε) conditions (Fardis, 1977). We symbolize this probability by $P(d|DA, \sigma, \varepsilon)$.

3. Number and Length of Liner Cracks for a Known Stress Field

The numerical results reveal that only the upper tail of the probability of sizes contributes to the probability of crack propagation from a Class 6 defect. Flaws in the upper tail of Class 6 sizes are rare enough to allow us to make the assumption of spatial independence of their occurrences, of their relative sizes, and of the local material toughness (as expressed by the NDTT). Therefore, conditionally on a given stress and strain field over the entire liner membrane, the only possible cause of dependence of crack initiations from different points is the common liner temperature T at the time of the seismic event. As the variability of this random variable is significantly smaller than the variability of the others, we can neglect the environmental dependence induced by it and we can state that the total number of failures (i.e., crack propagations) in the liner (conditionally on the stress and strain fields $\hat{\sigma}$, and $\hat{\varepsilon}$) is Poisson distributed with parameter $\nu(\hat{\sigma}, \hat{\varepsilon})$ equal to:

$$\nu(\hat{\sigma}, \hat{\varepsilon}) = \int_A \left(\int_{F_{D,DA}} n[P(b|D, \sigma) + P(d|DA, \sigma, \varepsilon)] P_6 dF_{D,DA} \right) dA \qquad (2)$$

where P_6 is the (per "reference length") mean rate of occurrence of Class 6 defects after inspection and repair, n is the number of weld "reference lengths" per unit liner surface, A symbolizes the entire liner surface and $F_{D,DA}(\cdot, \cdot)$ is the probability distribution of the defect size characteristics D and DA which enter the failure criteria above.

4. Stress Field for a Known Seismic Event

The stress ($\hat{\sigma}$) and the strain ($\hat{\varepsilon}$) fields on which the previous results are conditioned, are the envelope to all instantaneous stress and strain fields over the liner surface, that take place during a seismic event.

Presently available sophisticated analysis methods can be used to obtain the envelope $\hat{\sigma}$ and $\hat{\varepsilon}$ fields caused by a seismic event. The method used in this study is an approximate one, but it is simple enough to allow for the explicit incorporation of uncertainty (both probabilistic and statistical). Nevertheless the accuracy of the method is believed to be commensurate with the accuracy of the other parts of this study.

The simple models used for the determination of the envelope stress and strain fields are described briefly.

The containment structure is modeled as a cantilever beam with uniformly distributed mass, shear rigidity and bending rigidity, fixed at its base (i.e., soil-structure interaction effects are neglected). Only the two horizontal components of the ground motion are considered and the effect of the size of the base on the input motion is neglected (i.e., the input motion is considered as the free-field ground motion). The fundamental lateral vibrational mode only is taken into account.

Under the action of a ground motion with intensity considerably above the SSE level, extensive plastic action will develop in the (reinforcing or prestressing) steel and in the liner, especially at the lower part of the containment. In the presence of plastic action the shear and bending lateral stiffness of the pre-cracked containment will be reduced. The resulting nonlinearity, however, is not drastic. Furthermore, the reduction in stiffness is not enough to force the fundamental mode frequency out of the amplified acceleration frequency band of the Response Spectrum. (This is true even if we take into account the soil-structure interaction effects, at least for the firm ground on which a containment is typically founded.) Therefore, there is considerable justification for relating the maximum acceleration of a unidirectional ground motion imparted through one of the horizontal degrees of freedom of the base, to the resulting first mode response spectral acceleration by the (frequency-independent) acceleration amplification factor suggested by Newmark (1975). This amplification factor is a random variable, considered here lognormally distributed, with moments given by Newmark (1975) as a function of the damping ratio.

Containment structures are typically axisymmetric (e.g., they are composed of a cylindrical part capped by a dome). For these axisymmetric structures, then, a unidirectional horizontal ground motion will result in a response symmetrical with respect to the vertical plane through the ground motion's direction (i.e., the response is also "unidirectional"). The stresses and strains of this "unidirectional" response can be related to the corresponding spectral acceleration S_a in the following way: for given S_a, the overturning moment, the gross shear force, and the response acceleration at each elevation on the structure, can be determined from the first modal shape alone. A structure with very small shear rigidity (called a "shear-beam") will have a first mode shape different than that of a structure with very small bending rigidity (called here a "cantilever-beam"). Therefore, the resulting overturning moment, etc. distribution will be different. The overturning moment, overall normal force, etc. at a given elevation can also be distributed over the horizontal cross-section of the structure (i.e., up to the level of stresses is a specific component at a certain point on the periphery) in several different ways. An obvious one results from assuming that the overall behavior is in stretching. The problem becomes then statically determinate, and stresses at any point can be determined without resorting to deformation considerations. We will refer to this model as the "shell-model". A second model for the determination of stresses results from the observation that the dome is stiff enough to prevent the warping of the horizontal cross-sections at the upper part of the cracked cylinder, in which the "shell-model" results. A model which takes this effect into account is one in which horizontal cross-sections of the cylinder remain plane. We will refer to this second model as the "beam-model".

We have, therefore, two dynamic models (which are essentially elastic models) and two

models for the determination of the stress distribution (which take into account any inelastic action). For given "unidirectional" response spectral acceleration S_a, the resulting four combined models yield four different stress (and strain) fields. If we denote these fields by $\hat{\sigma}_{ss}(S_a)$ for the combination of the "shear-beam" and the "shell" models, $\hat{\sigma}_{cb}(S_a)$ for the combination of the "cantilever-beam" and the "beam" models, etc., we assume that we can express the "exact" stress field $\hat{\sigma}$ as:

$$\hat{\sigma}(S_a,A_o,B_o) = (\bar{A}+A_o)(1-\bar{B}-B_o)\hat{\sigma}_{ss} + (\bar{A}+A_o)(\bar{B}+B_o)\hat{\sigma}_{cs} + (1-\bar{A}-A_o)(1-\bar{B}-B_o)\hat{\sigma}_{sb} + \\ + (1-\bar{A}-A_o)(\bar{B}+B_o)\hat{\sigma}_{cb} \qquad (3)$$

A_o and B_o are normally distributed random variables ($\sim N(0, 0.10^2)$), whereas $\bar{A}$ is a linear function of elevation expressing the fact that we give more "weight" to the "shell" ("beam") model at lower ("higher") elevations. $\bar{B}$ is a linear function of S_a, expressing the fact that for low values of S_a the shear and bending rigidity contribute equally to the containment lateral stiffness, whereas high S_a's reduce the shear rigidity much more than the bending rigidity.

As a result, we are describing the "unidirectional" response stress field in a way that takes into account the uncertainty about which of the four stress fields is appropriate. The structural model uncertainty is, therefore, reduced.

The next step consists in going from the unidirectional ground motion and response to the full two-dimensional horizontal ground motion and response.

The most common way of describing the two-dimensional horizontal ground motion is by the simultaneous ground acceleration time-histories ($a_y(t)$ and $a_z(t)$ in Fig. 2) recorded along the two instrumentation horizontal directions y and z. An alternative (but equivalent) way consists in giving the ground acceleration vector time-history (both magnitude $|a_g(t)|$ and direction $\theta(t)$). Fig. 2 shows schematicly part of such an acceleration vector time-history and Fig. 3 shows a sample $a_\theta(\theta)$ vs. θ plot, where $a_\theta(\theta)$ denotes the maximum (over time) acceleration vector magnitude along horizontal direction θ.

The response of such a stiff structure to the two-dimensional ground motion will follow (especially in the presence of high damping) the ground acceleration vector time-history closely enough to allow us to assume that:

The maximum spectral acceleration along direction θ (i.e., that giving rise to instantaneous response only in the vertical plane through direction θ) is related to $a_\theta(\theta)$, the maximum ground acceleration magnitude along θ, by an amplification factor with the same probability distribution as the acceleration amplification factor of a unidirectional ground motion.

Based on the fact that a "unidirectional" response causes a stress (and strain) field which is roughly sinusoidally distributed over the containment periphery, we conclude that in the two dimensional case the maximum spectral acceleration along any direction θ causes a sinusoidally distributed stress field in neighboring directions. An indication of the shape of the envelope stress field around the periphery is, therefore, given by the envelope of sinusoids fitted at each point of the $a_\theta(\theta)$ curve of the seismic event. The dotted piecewise sinusoidal curve in Fig. 3 reflects the typically observed fact that the envelope is dominated by a few extreme points of the $a_\theta(\theta)$ curve.

To simplify the analysis we substitute the swarm of the small sinusoids (i.e., the central part of Fig. 3) by a horizontal line approximation. We approximate then the envelope stress (and strain) field by the part caused by a unidirectional motion with maximum acceleration equal to the predominant peak acceleration $B_1 a_{pk}$ (where a_{pk} is the absolute maximum in the two recorded acceleration time-histories and B_1 is equal to 1.223 in Fig. 3) and by a direction-independent part equal to the effect (i.e., stress or strain) along its own direction of a unidirectional ground motion with maximum acceleration $B_1 B_2 a_{pk}$ (in Fig. 3, $B_1 B_2$ equals 0.825 and the latter direction-independent part is based on the dashed horizontal line at ordinate 0.825). The acceleration amplification factors A_{f_1} and A_{f_2} for these two unidirectional motions are joint lognormally distributed with moments given by Newmark (1975) and a correlation coefficient determined by Fardis (1977).

We just described a simple approximate way for the determination of the envelope stress and strain fields over the liner, caused by a seismic event described by $B_1 a_{pk}$ and $B_1 B_2 a_{pk}$. We want, however, to describe the seismic event by a single parameter. We choose here the peak recorded acceleration a_{pk} as this single quantity. (The average of the two orthogonal maximum accelerations along the instrumentation directions is an alternative choice, and it has also been pursued.) For this reason, the joint probability distribution $F_{B_1,B_2}(\cdot, \cdot)$ of B_1 and B_2 has been established (Fardis, 1977) based on the analysis of 24 seismic events.

5. Number and Length of Liner Cracks for a Known Seismic Event

The conclusion of the previous section was that the envelope stress and strain fields are approximately described if we specify the products $B_1 a_{pk}$ and $B_1 B_2 a_{pk}$, the acceleration amplification factors A_{f_1} and A_{f_2}, and the (structural model) random variables A_o and B_o. Symbolically:

$$\hat{\sigma} = \hat{\sigma}(B_1 a_{pk},\ B_1 B_2 a_{pk},\ A_{f_1},\ A_{f_2},\ A_o,\ B_o) \tag{4}$$

A similar expression holds for $\hat{\varepsilon}$.

We can obtain the probability distribution of the number of cracks N_c, conditional on a_{pk} only, from the probability distribution of N_c, conditional on $\hat{\sigma}$ and $\hat{\varepsilon}$, specified in section 3. Specifically:

$$F_{N_c|a_{pk}} = \int_{B_1}\int_{B_2}\int_{A_{f_1}}\int_{A_{f_2}}\int_{A_o}\int_{B_o} F_{N_c|\hat{\sigma},\hat{\varepsilon}}\, dF_{A_o}\, dF_{B_o}\, dF_{A_{f_1},A_{f_2}}(\cdot,\cdot)\, dF_{B_1,B_2}(\cdot,\cdot) \tag{5}$$

The total crack length L_t is equal to:

$$L_t = \sum_{i=1}^{N_c} L_i \tag{6}$$

where L_i is the random individual crack length. It is not an easy task to establish the probability distribution of L_i (conditional on the crack i propagation). Based on the fact that the crack will be arrested only if it enters a region in the propagation medium where a significantly lower stress exists, on the magnitude of the crack propagation velocity and on the vibrational frequency of the structure, we have chosen for any L_i a lognormal (conditional) distribution with mean equal to one third of the containment periphery and stan-

dard deviation equal to one ninth of it.

As far as the correlation of the L_1's (conditionally on crack propagation) is concerned, the individual crack lengths are very close to perfectly (positively) correlated, because they commonly (and strongly) depend on the details of the structural response.

6. Numerical Results

The analysis above has been applied to a typical PWR reinforced concrete containment. Fig. 4 shows the resulting probability distribution of the total number of cracks for several values of the peak recorded acceleration and for the case that the rejection of a weld test unit ℓ_u during inspection leads to full inspection of the unit (Event C_1 in Fig. 1). Fig. 5 shows the corresponding probability distribution for the case that the rejection results in rewelding of the unit (Event C_2). Fig. 6 shows the mean and standard deviation of the total crack length for both events C_1 and C_2. The standard deviation is shown for both the cases of individual crack lengths (conditionally) independent and (conditionally) perfectly correlated. The effect of the relative cost and of the resulting damage rates for the two different inspection procedures on the decision which one should be preferred, is beyond the scope of this paper.

7. Acknowledgement

This research has been sponsored by a grant from the Probabilistic Analysis Branch, Office of Nuclear Regulatory Research, U.S. N.R.C.

References

1. American Society of Mechanical Engineers, "ASME Boiler and Pressure Vessel Code," Section III, Division 2, Concrete Components in Nuclear Service, 1974.
2. Fardis, M. N., "A Reliability Study of Containment Resistance under Extreme Loads," M.S. Thesis, Department of Civil Engineering, Massachusetts Institute of Technology, January, 1977.
3. Kihara, H., Tada, Y., Watanabe, M. and Ishii, Y., "Nondestructive Testing of Welds and their Strength," 60th Anniversary Series, 7, The Society of Naval Architects of Japan, 1960.
4. Newmark, N. M., "A Response Spectrum Approach for Inelastic Seismic Design of Nuclear Reactor Facilities," Transactions, 3rd International Conference on Structural Mechanics in Reactor Technology, Vol. 4, Part K, Paper K5/1, London, U.K., September, 1975.
5. Pellini, W. S., "Principles of Fracture Safe Design," Welding Journal, Part I, March, 1971 and Part II, April, 1971.
6. Shabbits, W. O., "Dynamic Fracture Toughness Properties of Heavy Section A 533 Grade B Class 1 Steel Plate," Westinghouse Electric Corporation, WCAP-7623, December, 1970.
7. Shoemaker, A. K. and Rolfe, S. T., "Static and Dynamic Low Temperature K_{IC} Behavior of Steels," Transactions of the American Society of Mechanical Engineers, Journal of Basic Engineering, September, 1969.

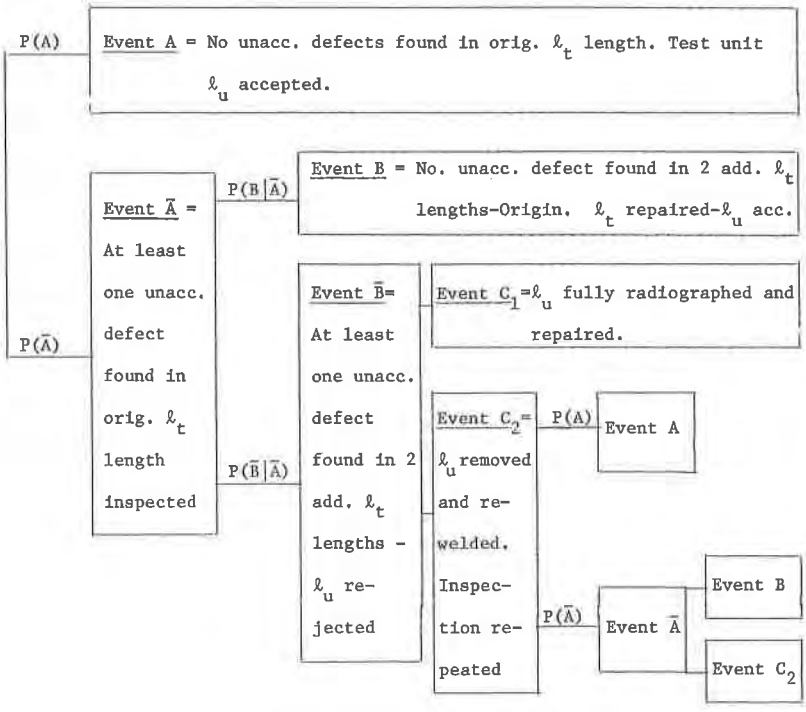

Fig. 1 Event tree for the A.S.M.E. Radiographic inspection procedure, applied to a single weld test unit ℓ_u

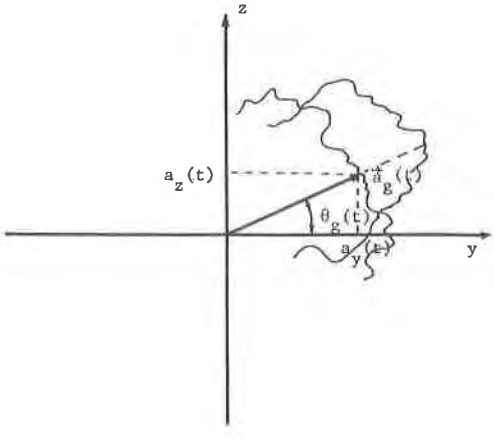

Fig. 2 Description of an acceleration time history

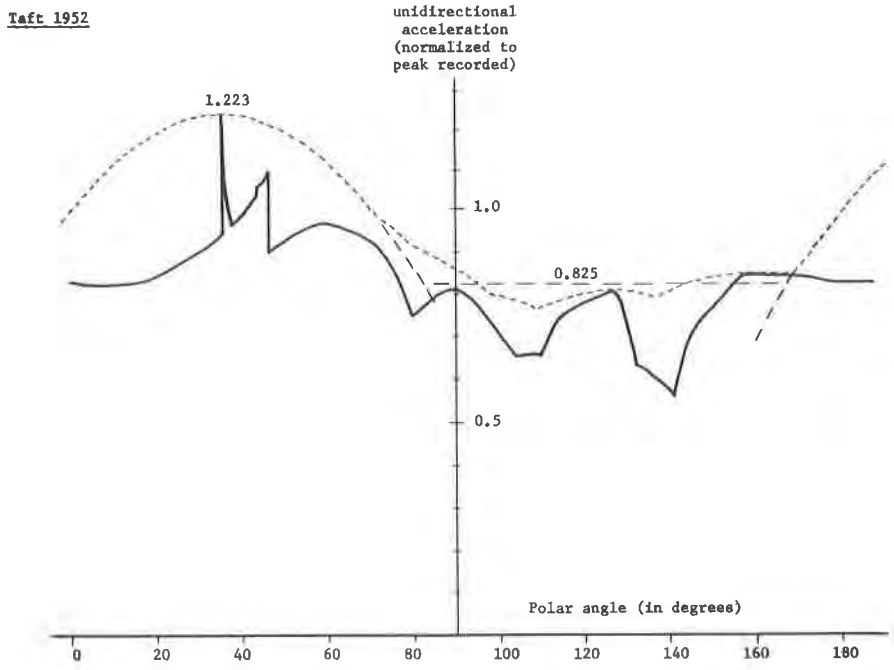

Fig. 3 Unidirectional ground maximum acceleration vs. direction.

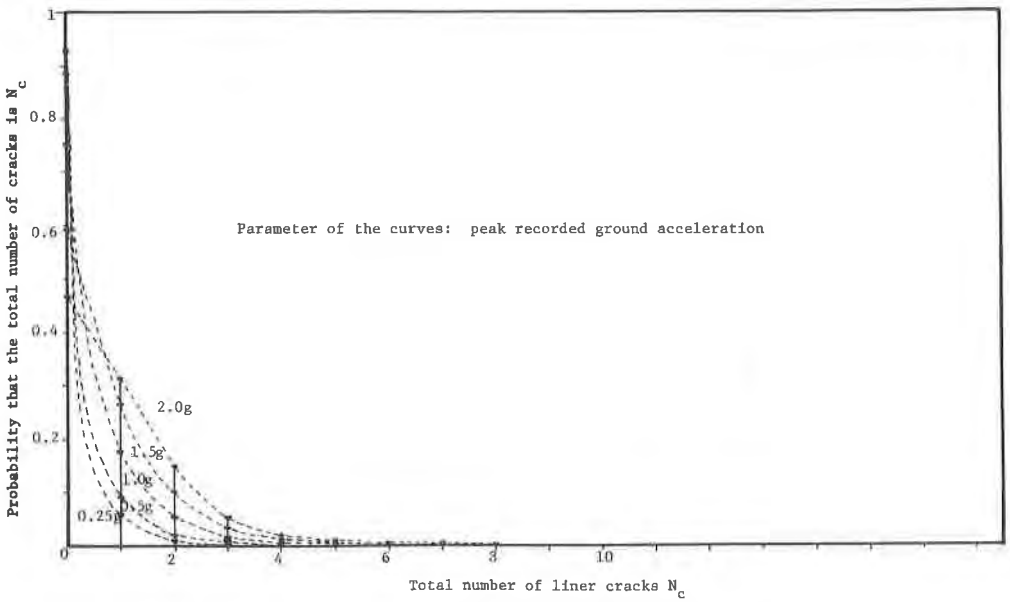

Fig. 4 Probability distribution of total number of cracks in the liner. Rejected test units are fully inspected (Event C_1).

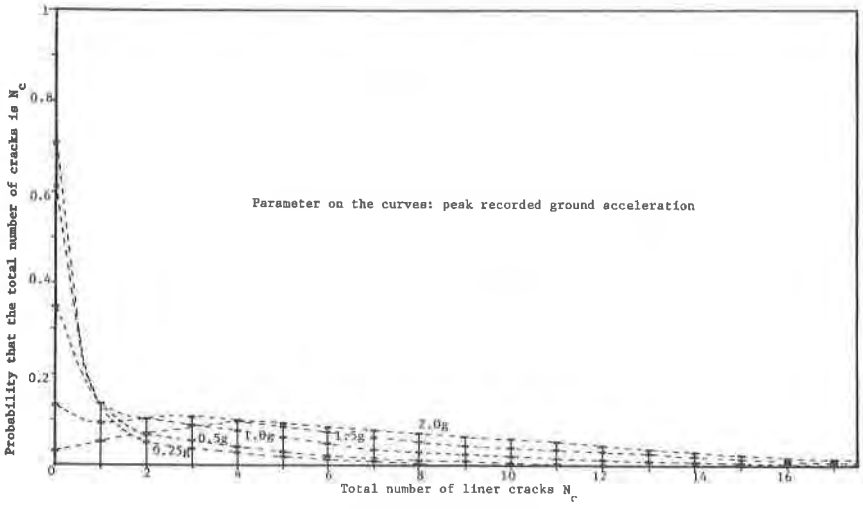

Fig. 5 Probability distribution of total number of cracks in the liner. Rejected weld test units are rewelded (Event C_2).

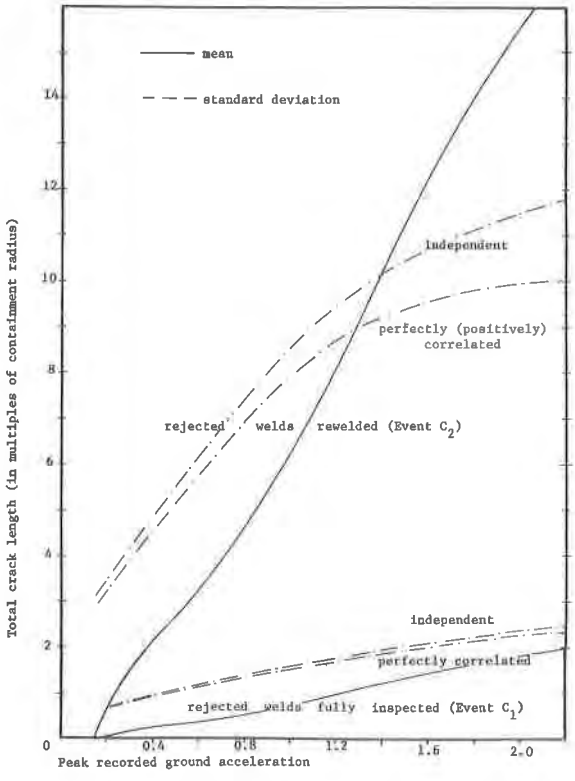

Fig. 6 Total liner crack length mean and standard deviation vs. peak recorded ground acceleration.